ARTICLE

Density Functional Theory Study of Infrared and Ultraviolet Spectra of Urea L-Malic Acid

Yan-lan Zhang[a], Hong-yan Wang[b*], Dong-sheng Jiao[a], Yong-hong Hu[c]

a. Institute of Atomic and Molecular Physics, Sichuan University, Chengdu 610065, China
b. College of Sciences, Southwest Jiaotong University, Chengdu 610031, China
c. College of Life Science and Pharmaceutical Engineering, Nanjing University of Technology, Nanjing 210009, China

(Dated: Received on June 26, 2008; Accepted on September 5, 2008)

Urea L-malic acid, a new second order nonlinear optical crystal, was studied using density functional theory (DFT). PBEPBE/6-31+G(d,p) method, the optimal method for comparing the results from the several DFT methods, was chosen to study the molecular structure. Infrared and ultraviolet-visible spectra were obtained and compared with experiments. The ultraviolet-visible spectrum was also analyzed by the molecular orbital population. The geometries, and the infrared and ultraviolet-visible spectra in water were studied using DFT methods in combination with the polarized continuum model to predict the perturbations by the solvent effect.

Key words: Urea L-malic acid, Density functional theory, Molecular structure, Infrared spectrum, Ultraviolet-visible spectrum

I. INTRODUCTION

New nonlinear optical crystals have been actively studied because of their increased demand for use in communication, sensing and instrumentation [1]. Organic crystals exhibit quadratic nonlinear efficiencies many times larger than those of conventional inorganic crystals [2-5]. Recently organic inclusion complex (OIC), one type of these materials, has been popular and become used in ultraviolet frequency doublers.

Urea L-malic acid (ULMA), $CO(NH_2)_2C_4H_6O_5$, one such OIC molecular crystal, was reported to exhibit second harmonic efficiency three times that of the widely used inorganic crystal, potassium dihydrogen phosphate at the fundamental wavelength of 1064 nm, and kept the nonlinear optical properties and broad transparency range of urea with greatly reduced hygroscopicity. Its transparency range was from 380 nm to 1440 nm and its second harmonic generation (SHG) efficiency was roughly three times greater than that of the inorganic compound KDP [6,7]. L-malic acid, used as a means for creating two-dimensional anionic networks held together by $O-H\cdots O$ hydrogen bonds, has been demonstrated to be a suitable anionic building block for synthesizing the compound ULMA. The crystal structure consists of urea and L-malic acid molecules resulting in a complex two-dimensional hydrogen bond framework [8]. ULMA has been synthesized [6,7], and its structure has been determined by X-ray single crystal diffraction [6,7,9]. The characteristics of ULMA film and powder, including infrared spectrum (IR), ultraviolet-visible (UV-Vis) spectrum, have been reported in Ref.[9]. Crystals of ULMA have been grown by solvent evaporation technique at ambient temperature using different solvents like water, methanol, and ethanol. Optical transmittance was found to be larger for crystals grown from water. Both the dielectric constant and dielectric loss varied slowly with frequency [10]. Theoretical studies on the molecular structure of ULMA were performed in this work to predict its IR and UV-vis spectrum to determine the characteristic peak. The characterization of ULMA in water was studied to compare with recent experiments.

II. COMPUTATIONAL METHODS

All computations were performed with the GAUSSIAN 03W series of programs [11]. The equilibrium geometries of the molecule were optimized by the density function: B3LYP [12-14], mPW1PW [15-17], BPW91 [12,18,19], PBEPBE [20,21], and BP86 [12,22]. Of these, B3LYP and mPW1PW are hybrid DFT methods, while BPW91, PBEPBE, and BP86 are pure DFT methods. The force constants and vibrational frequencies were determined at the stationary point to check if they were true minima. The polarizable continuum models (PCM) took account of specific molecular shape in the construction of the solute cavity [23-25]. The solvent chosen in our work was water. The basis sets used in this work were 6-31+G(d,p) and 6-311+G(d,p) [26,27].

The calculation of the UV-vis spectrum of ULMA has been performed by solving the time dependent Kohn-Sham equations according to the method implemented

*Author to whom correspondence should be addressed. E-mail: wanghyxx@yahoo.com

TABLE I Bond distances (in unit of Å) and bond angles (in unit of (°)) for the ULMA at the different DFT/6-31+G(d,p) level.

Bond distance or angle	B3LYP	mPW1PW	BPW91	PBEPBE	Experiment [6]
O1−C9	1.219	1.215	1.228	1.228	1.258
O2−C10	1.324	1.316	1.331	1.328	1.309
O3−C10	1.224	1.221	1.237	1.239	1.209
O4−C11	1.406	1.396	1.412	1.409	1.407
O5−C13	1.217	1.213	1.224	1.228	1.206
O6−C13	1.345	1.336	1.357	1.354	1.316
N7−C9	1.424	1.416	1.438	1.438	1.330
N8−C9	1.366	1.359	1.372	1.370	1.330
C10−C11	1.528	1.416	1.535	1.533	1.520
C11−C12	1.536	1.527	1.416	1.541	1.513
C12−C13	1.513	1.505	1.517	1.514	1.497
O1−C9−N7	121.5	121.5	121.5	121.4	120.3
O1−C9−N8	124.7	124.8	125.1	125.2	121.0
N7−C9−N8	113.8	113.8	113.4	113.4	118.6
O2−C10−O3	125.3	125.4	125.6	125.7	124.7
O2−C10−C11	113.9	114.14	114.2	114.3	111.7
O3−C10−C11	120.8	120.5	120.2	120.0	123.4
O4−C11−C10	109.6	109.5	109.4	109.4	112.0
O4−C11−C12	110.0	110.2	110.5	110.5	108.8
C10−C11−C12	112.9	110.9	119.2	111.9	114.6
C11−C12−C13	112.1	109.7	112.1	111.6	115.6
O5−C13−O6	122.1	122.3	122.1	122.1	123.1
O5−C13−C12	125.4	125.2	125.7	125.7	125.7
O6−C13−C12	112.4	112.5	112.2	112.2	111.2

in GAUSSIAN 03W [11]. The oscillator strengths are very helpful in assigning the calculated electronic transitions to experimental absorption and emission bands. In this work the oscillator strengths, f, were calculated by the TD-DFT method. The IR and UV-Vis spectra were calculated and visualized using the SWizard program [28].

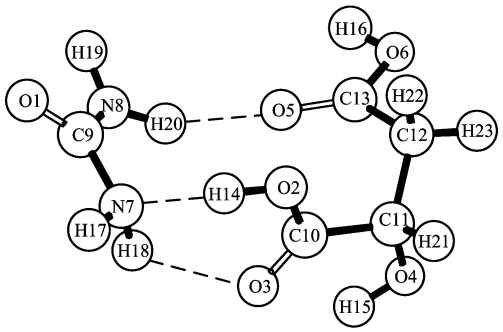

FIG. 1 Molecular structure of the ULMA molecule calculated by PBEPBE/6-31+G(d,p).

III. RESULTS AND DISCUSSION

A. Geometries

The equilibrium conformation of the neutral molecule of ULMA calculated by B3LYP, mPW1PW, BPW91, and PBEPBE methods with the basis set 6-31+G(d,p) are reported in Table I. The molecular structure with the atomic label and number is shown in Fig.1. The optimized results showed that the nonplanar ULMA had no symmetry at the ground state both in pure DFT and hybrid DFT, and it was very interesting to find there was no symmetry for the urea in the ULMA, whereas in the gas phase, nonplanar structure of C_2 symmetry of urea had been experimentally indicated by microwave spectroscopy [29].

The optimized results were compared with the experimental values of ULMA determined by X-ray single crystal diffraction [6], and they were in good agreement with the experiments. The standard errors for the interatomic bond distances were 0.0374/B3LYP, 0.0349/mPW1PW, 0.0510/BPW91, 0.0314/PBEPBE, and the standard errors for the bond angles were 2.54/B3LYP, 3.73/mPW1PW, 3.00/BPW91, and 2.91/PBEPBE. Pure DFT and hybrid DFT method had almost the same standard error for bond distances and angles; however PBEPBE method was

DOI:10.1088/1674-0068/21/06/535-540

TABLE II IR frequencies (in unit of cm^{-1}) for the ULMA with pure DFT and hybrid DFT chemical model.

	B3LYP/ 6-31+G(d,p)	mPW1PW/ 6-31G+(d,p)	BPW91/ 6-31G+(d,p)	PBEPBE/ 6-31G+(d,p)	PBEPBE/ 6-311+G(d,p)	Experiment [9]
ν(CO)	1787, 1821, 1844	1821, 1856, 1878	1719, 1760, 1795	1720, 1763, 1801	1706, 1749, 1783	1721
$\nu_s(NH_2)$	3485, 3561	3524, 3605	3386, 3467	3366, 3455	3374, 3457	3358
$\nu_{as}(NH_2)$	3625, 3708	3675, 3761	3545, 3634	3537, 3628	3526, 3610	3484

better than other methods according to the following vibrational frequencies calculation. The distances of the three intermolecular hydrogen bonds for N7−H18···O3, O5···H20−N8, and N7···H14−O2 in PBEPBE/6-31+G(d,p) were 2.17, 2.08, and 1.68 Å respectively. In contrast, only two intermolecular hydrogen bonds, i.e. 2.17 Å N7−H18···O3 and 2.39 Å O5···H20−N8, were predicted by Gomes [6]. The bond distances and bond angles adjoining the hydrogen bonds usually deviated largely from experimental values, i.e. O1−C9−N8, N7−C9−N8, O2−C10−C11, O3−C10−C11, O4−C11−C10, and C10−C11−C12.

B. Vibrational frequencies and IR spectrum

The vibrational frequencies of ULMA are listed in Table II. The pure DFT methods were better than hybrid DFT methods. The vibrational frequencies, whether the carbonyl stretching vibration or symmetrical and asymmetrical stretching vibration of amino groups, evidently were overestimated by the hybrid DFT (B3LYP, mPW1PW) methods compared with the experiments. The PBEPBE method was a little better than BPW91 method, especially at absorption peaks of 1720 and 3366 cm^{-1}, which were very close to the experimental values. The computed values of $\nu_s(NH_2)$ and ν(CO) in the PBEPBE method with the basis set 6-311+G(d,p) were a little closer to the experimental values than in the PBEPBE/6-31+G(d,p) method, and considering the numbers of basis functions and the computing time, the PBEPBE/6-31+G(d,p) method was chosen to calculate the ULMA spectrum. The molecular dipole moment with PBEPBE/6-31+G(d,p) is 2.15 Debye, the calculated molecular volume is 146.679 cm^3/mol.

The IR spectrum for the ULMA molecule calculated with PBEPBE/6-31+G(d,p) is displayed in Fig.2(a), and the principal peaks are shown without any scaling. 1720, 1763, and 1801 cm^{-1} was assigned to C10−O3 stretching vibration, C13−O5 stretching vibration in L-malic acid, and C9−O1 stretching vibration in urea respectively. An intense band at 1721 cm^{-1} assigned to the carbonyl stretching vibration was observed by using ULMA crystal grown from aqueous solution [7]. 3366, 3455, 3537, and 3628 cm^{-1} with the symmetrical and asymmetrical stretching vibration from amino groups were observed; 3366 and 3455 cm^{-1} corresponded to H17−N7−H18 and H19−N8−H20 symmetrical stretching vibration, while 3537 and 3628 cm^{-1} were assigned to H17−N7−H18 and H19−N8−H20 asymmetrical stretching vibration accordingly. Intense bands at 3356 and 3482 cm^{-1} indicating the asymmetrical and symmetrical stretching vibration from amino groups were also observed [7]. 3484, 3358, and 1721 cm^{-1} were observed by using ULMA film [9]. The calculated values were very close to the experiments. The new intense band at 2682 cm^{-1} was found to be assigned to the strong O2−H14 stretching vibration, which was probably the hydrogen bond N7···H14−O2.

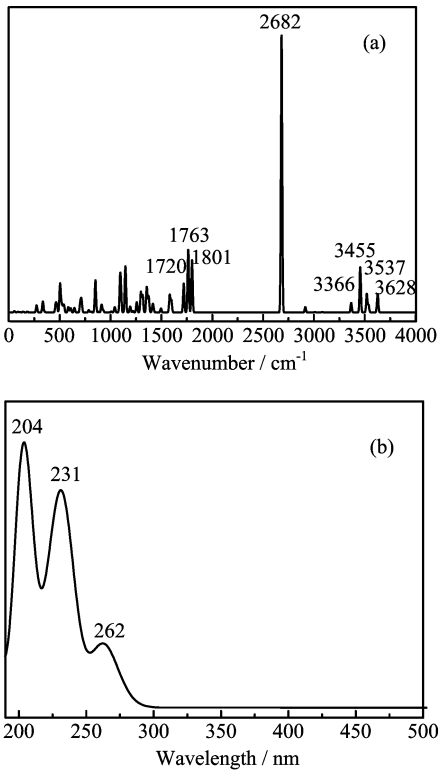

FIG. 2 (a) IR spectrum and (b) UV-Vis spectrum of the ULMA molecule calculated with PBEPBE/6-31+G(d,p).

C. UV-Vis spectrum

The UV-Vis spectrum of the ULMA molecule calculated with PBEPBE/6-31+G(d,p) is displayed in Fig.2(b). The same trend between the calculated and experimental spectra is observed. Three absorption peaks were predicted at the range of 200-300 nm in

DOI:10.1088/1674-0068/21/06/535-540

TABLE III Computed absorption wavelengths, excitation energies, molecule orbitals and oscillator strengths of ULMA at the TD-DFT/6-31+G(d,p) level.

Wavelength/nm	Excitation energy/eV	Molecule orbital	Oscillator strength
204	5.27	HOMO→LUMO+2	0.0024
231	5.31	HOMO−1→LUMO+1	0.0073
258	4.81	HOMO→LUMO+1	0
262	4.69	HOMO−1→LUMO	0.0031
290	4.27	HOMO→LUMO	0

calculation, however the oscillator strength of the electronic transitions was very low, less than 0.01, which could not be obviously observed in the experiment. The predicted peaks could be confirmed by orbital analysis.

The contour plots of the frontier orbitals for the ground state of ULMA molecule are shown in Fig.3 including the highest occupied molecular orbital (HOMO), second occupied molecular orbital (HOMO−1), lowest unoccupied molecule orbital (LUMO), second unoccupied molecule orbital (LUMO+1) and third unoccupied molecule orbital (LUMO+2). It is interesting to see the orbital population change from HOMO to LUMO and LUMO+1. In the HOMO, the electron densities are substantially distributed over the urea molecule, while in the others, over the L-malic acid molecule. The oscillator strength f of HOMO→LUMO and HOMO→LUMO+1 transitions is zero, meaning that the electron transition is not permitted. The electron transition from HOMO to LUMO+2 leads to the 204 nm absorption peak, while HOMO−1→LUMO+1 and HOMO−1→LUMO lead to the 231 and 262 nm absorption peak respectively, as shown in Table III.

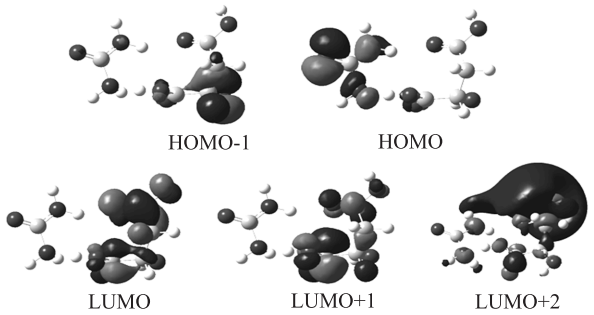

FIG. 3 Molecular orbital surfaces of the HOMO−1, HOMO, LUMO, LUMO+1, and LUMO+2 for the ground-state of ULMA.

D. Solvent effect

According to the molecular dipole moment of ULMA in the gas, this molecule is a relatively polarized system and can be solubilized in polar solvents such as water and ethanol, which has been reported in Ref.[10]. The size of molecular volume is important to determine if a molecule will fit in the active site of an enzyme, or for establishing the cavity size for solvation calculations [30].

The BP86/6-31+G(d,p) method was used to optimize the geometries of ULMA molecule in water. During the search for minima, because the numerical integration procedures used in existing DFT methods had significant limitations, when one predicts an imaginary vibrational frequency of magnitude less than 100 cm^{-1}, the conclusion should be that there is a minimum of energy identical to or close to that of the stationary point in question. Accordingly, we did not in general follow the imaginary eigenvector in search of another minimum in such cases.

The equilibrium geometries of the ULMA in the water was compared with the results in the gas, indicating there was no obvious change, except the H20−N8, H14−O2, O1−C9−N8, O2−C10−C11, O3−C10−C11, and O5−C13−C12 because of the perturbations by the solvent effect on the hydrogen bonds. There were only two hydrogen bonds O5$\cdots$H20−N8 and N7$\cdots$H14−O2 existing in the water. The hydrogen bond between H18 and O3 does not exist in the water because the geometries were distorted by the solvent effect.

The IR spectrums of the ULMA in gas and water are shown in Fig.4(a), without any scaling of the principal peaks. Their main intense bands in water evidently red shift, and their absorbances are stronger compared with ones in gas. The frequencies of ν(CO), $\nu_s(NH_2)$, and $\nu_{as}(NH_2)$ in water were lower than ones in gas accordingly. Because the hydrogen bond distances decreased in the water (specifically, 0.07 Å shorter in water than in gas for O5$\cdots$H20−N8, 0.03 Å shorter for N7$\cdots$H14−O2) the shifts of protons in O5$\cdots$H20−N8 and N7$\cdots$H14−O2 in water were much easier than ones in gas, leading to the bonds of H20−N8, H14−O2 becoming long, so the corresponding stretching vibrations in water would be lower than in gas. In the gas phase the C9−O1, C10−O3, and C13−O5 stretching vibration was calculated to absorb at 1801, 1720, and 1763 cm^{-1}, and in the solution spectrum these vibrations were assigned to the band at 1724, 1691, and 1704 cm^{-1}, which appeared at 1721 cm^{-1} in the solid state spectrum. It was found that the frequencies in gas were much larger than ones in water. The same phenomenon existed in the $\nu_s(NH_2)$ and $\nu_{as}(NH_2)$, so

DOI:10.1088/1674-0068/21/06/535-540

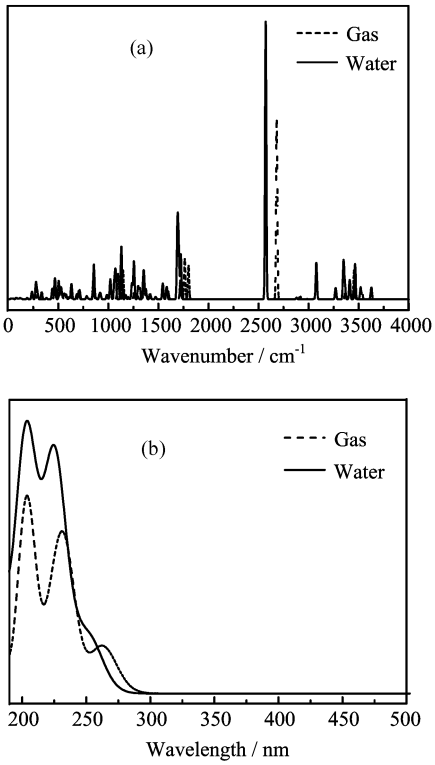

FIG. 4 (a) IR spectrum and (b) UV-Vis spectrum of the ULMA molecule calculated with DFT/6-31+G(d,p) in gas and water.

it can be concluded that a ULMA in solution was not an intermediate state between the solid state and the gas phase.

The UV-Vis spectra of the ULMA in gas and water are shown in Fig.4(b). Two absorption peaks at the range of 200-250 nm were observed in water, and three absorption peaks in gas. No absorption peak was observed below 200 nm both in the calculation and in the experiment [10] for the ULMA water solvent. The wavelengths of the absorption peaks in water were 203 and 226 nm, which are lower than ones in gas, 204 and 231 nm, but the absorbances in water were stronger than ones in gas. The absorption peak at 262 nm in gas disappeared in water.

IV. CONCLUSION

In this work, density functional theory was used to study the molecular structure of ULMA in the gas phase and in the water solvent. The total energy and the dipole moment were displayed. The calculated molecular volume for the molecule is also reported. The pure DFT methods were found to be better than hybrid DFT methods. The IR absorption band predicted by DFT was very similar to the experiment except at the intense band at 2682 cm^{-1}, which was probably because of the effect of hydrogen bond N7$\cdots$H14$-$O2. The UV-Vis spectrum of ULMA was predicted by using the TD-DFT, and three absorption peaks were predicted at the range of 200-300 nm in UV-Vis spectrum, corresponding to the electron transitions from the HOMO to LUMO+2, the HOMO$-$1 to LUMO+1, and the HOMO$-$1 to LUMO. However, due to their oscillator strength of the electronic transitions being less than 0.01 Å, no obvious absorption band was observed in the experiment. The IR spectrums of the ULMA in gas and water showed that the main intense bands in water evidently red shifted, and their absorbance were stronger compared with ones in gas. Accordingly, the frequencies of ν(CO), $\nu_s(NH_2)$ and $\nu_{as}(NH_2)$ in water were lower than in gas. Because the hydrogen bond distances decreased in the water (0.07 Å shorter in water than in gas for O5$\cdots$H20$-$N8, about 0.03 Å shorter for N7$\cdots$H14$-$O2) the shifts of protons in O5$\cdots$H20$-$N8 and N7$\cdots$H14$-$O2 in water were much easier than ones in gas, and the corresponding stretching vibrations in water were lower than in gas. The structure of ULMA and its IR and UV-Vis spectrum in the water were perturbed by the solvent effect. The number of hydrogen bonds decreased and the absorption peaks in UV-Vis spectrum became stronger. The red shift was observed in the IR spectrum in the water.

V. ACKNOWLEDGMENTS

This work was supported by the Program for New Century Excellent Talents in University, the Science and Technology Foundation for Young Scholars in Sichuan Province, and the National Natural Science Foundation of China (No.10774104).

[1] D. F. Eaton, Science **253**, 281 (1991).
[2] J. Zyss, J. F. Nicoud, and M. Loquillay, J. Chem. Phys. **81**, 4160 (1984).
[3] S. R. Marder, J. W. Perry, and W. P. Schaefer, Science **245**, 626 (1989).
[4] H. Yamamoto, S. Funato, and T. Sugiyama, J. Opt. Soc. Am. B **13**, 837 (1996).
[5] S. Follonier, C. Bosshard, and U. Meier, J. Opt. Soc. Am. B **14**, 593 (1997).
[6] E. de Matos Gomes, V. Venkataramanan, E. Nogueira, M. Belsley, F. Proenca, A. Criado, M. J. Dianez, M. J. Dianez, M. D. Estrada, and S. Perez-Garrido, Synth. Met. **115**, 225 (2000).
[7] V. K. Dixit, S. Vanishri, H. L. Bhat, E. de Matos Gomes, M. Belsley, C. Santinha, G. Arunmozhi, V. Venkataramanan, F. Proena, and A. Criado, J. Cryst. Growth **253**, 460 (2003).
[8] C. B. Aakeroy and M. Nieuwenhuyzen, J. Chem. Soc. Chem. Commun. **116**, 10983 (1993).
[9] L. Zhu, J. Y. Zhang, D. A. Chen, X. Y. Feng, Y. H. Hu, L. L. Xu, W. Wang, and Y. P. Cui, Mater. Lett. **60**, 1740 (2006).

DOI:10.1088/1674-0068/21/06/535-540

[10] S. Moitra and T. Kar, Mater. Lett. **62**, 1609 (2008).
[11] M. J. Frisch, G. W. Trucks, H. B. Schlegel, G. E. Scuseria, M. A. Robb, J. R. Cheeseman, J. A. Montgomery, Jr., T. Vreven, K. N. Kudin, J. C. Burant, J. M. Millam, S. S. Iyengar, J. Tomasi, V. Barone, B. Mennucci, M. Cossi, G. Scalmani, N. Rega, G. A. Petersson, H. Nakatsuji, M. Hada, M. Ehara, K. Toyota, R. Fukuda, J. Hasegawa, M. Ishida, T. Nakajima, Y. Honda, O. Kitao, H. Nakai, M. Klene, X. Li, J. E. Knox, H. P. Hratchian, J. B. Cross, C. Adamo, J. Jaramillo, R. Gomperts, R. E. Stratmann, O. Yazyev, A. J. Austin, R. Cammi, C. Pomelli, J. W. Ochterski, P. Y. Ayala, K. Morokuma, G. A. Voth, P. Salvador, J. J. Dannenberg, V. G. Zakrzewski, S. Dapprich, A. D. Daniels, M. C. Strain, O. Farkas, D. K. Malick, A. D. Rabuck, K. Raghavachari, J. B. Foresman, J. V. Ortiz, Q. Cui, A. G. Baboul, S. Clifford, J. Cioslowski, B. B. Stefanov, G. Liu, A. Liashenko, P. Piskorz, I. Komaromi, R. L. Martin, D. J. Fox, T. Keith, M. A. Al−Laham, C. Y. Peng, A. Nanayakkara, M. Challacombe, P. M. W. Gill, B. Johnson, W. Chen, M. W. Wong, C. Gonzalez, and J. A. Pople, *Gaussian* 03 (*Revision B*.02), Pittsburgh, PA: Gaussian, Inc., (2003).
[12] A. D. Becke, Phys. Rev. A **38**, 3098 (1988).
[13] C. Lee, W. Yang, and R. G. Parr, Phys. Rev. B **37**, 785 (1988).
[14] B. Miehlich, A. Savin, H. Stoll, and H. Preuss, Chem. Phys. Lett. **157**, 200 (1989).
[15] C. Adamo and V. Barone, J. Chem. Phys. **116**, 5933 (2002).
[16] K. Burke, J. P. Perdew, and Y. Wang, *in Electronic Density Functional Theory: Recent Progress and New Directions*, J. F. Dobson, G. Vignale, and M. P. Das, Ed., New Youk: Plenum, (1998).
[17] C. Adamo and V. Barone, J. Chem. Phys. **108**, 664 (1998).
[18] J. P. Perdew, J. A. Chevary, S. H. Vosko, K. A. Jackson, M. R. Pederson, D. J. Singh, and C. Fiolhais, Phys. Rev. B **48**, 4978 (1993).
[19] J. P. Perdew, K. Burke, and Y. Wang, Phys. Rev. B **54**, 16533 (1996).
[20] J. P. Perdew, K. Burke, and M. Ernzerhof, Phys. Rev. Lett. **77**, 3865 (1996).
[21] J. P. Perdew, K. Burke, and M. Ernzerhof, Phys. Rev. Lett. **78**, 1396 (1997).
[22] J. P. Perdew, Phys. Rev. B **33**, 8822 (1986).
[23] S. Miertus, E. Scrocc, and J. Tomasi, Chem. Phys. **55**, 117 (1981).
[24] S. Miertus and J. Tomasi, Chem. Phys. **65**, 239 (1982).
[25] M. Cossi, V. Barone, R. Cammi, and J. Tomasi, Chem. Phys. Lett. **255**, 327 (1996).
[26] J. B. Foresman and E. Frisch, *Exploring Chemistry with Electronic Structure Methods*, 2nd, Pittsburgh, PA: Gaussian Inc., (1996).
[27] J. A. Montgometry Jr., M. J. Frisch, J. W. Ochterski, and G. A. Petersson, J. Chem. Phys. **110**, 2822 (1999).
[28] S. I. Gorelsky, SWizard Program, revision 4.5, 2008, http://www.sg-chem.net/swizard/.
[29] A. Masunov and J. Dannenberg, J. Phys. Chem. **103**, 178 (1999).
[30] D. Young, *Computational Chemistry-A Practical Guide for Applying Techniques to Real World Problems*, New York: Wiley, (2001).

DOI:10.1088/1674-0068/21/06/535-540